Electronic Supplementary Material (ESI) for ChemComm.

Supporting Information

New M- and V-shaped Perylene Diimide Small Molecules for High-Performance Nonfullerene Polymer Solar Cells

Gi Eun Park†, Hyung Jong Kim†, Suna Choi, Dae Hee Lee, Mohammad Afsar Uddin, Han Young Woo, Min Ju Cho* and Dong Hoon Choi*

E-mail: chominju@korea.ac.kr, dhchoi8803@korea.ac.kr

1. Experimental

All commercial reagents and solvents were purchased from Tokyo Chemical Industry (TCI), Alfa Aesar, Sigma-Aldrich, and Acros Organics. The 4,4'-(cyclohexane-1,1-diyl)dianiline (**M1**),[1] monobrominated phenylene diimide (**M4**),[2] and perylene monoimido anhydride (**M5**)[3] were synthesized following modified literature procedures.

1.1 Synthesis

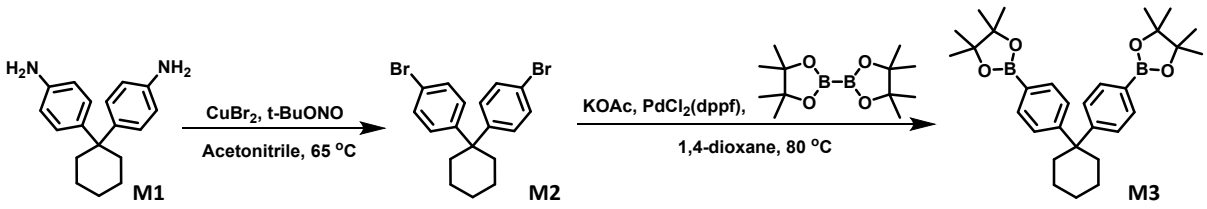

Scheme S1 Synthesis of the V-shape core.

Synthesis of 4,4'-(cyclohexane-1,1-diyl)bis(bromobenzene), M2 [4]

4,4'-(Cyclohexane-1,1-diyl)dianiline (2 g, 7.5 mmol) (1) was dissolved to 35 mL of degassed acetonitrile in a 100 mL two-neck round bottom flask. $CuBr_2$ (3.79 g, 1.7 mmol) and *t*-butyl nitrite (*t*-BuONO) (1.75 g, 17 mmol) were subsequently added to the mixture. The flask was protected from light and stirred under a nitrogen atmosphere at 65 ^{o}C for 6 h. The solvent mixture was removed by evaporation and the residue was extracted with methylene chloride (MC) and water. The organic phase was dried with sodium sulfate and concentrated. The residue was purified by column chromatography (eluent : MC : hexane = 1 : 2 v/v) to obtain the product at a 64% yield (1.90 g). ^{1}H NMR (400 MHz, $CDCl_3$) δ (ppm): 8.89 (d, *J* = 4.3 Hz, 2H), 7.06 (d, *J* = 3.92 Hz, 2H), 7.02 (d, *J* = 3.92 Hz, 2H), 4.02 (d, 4H), 1.94 (m, 2H), 1.15-1.4 (m, 48H), 0.8-0.9 (m, 12H). Anal. Calcd for $C_{18}H_{18}Br_2$: C, 54.85; H, 4.60; Br, 40.55. Found: C, 54.24; H, 4.82; Br, 40.94.

Synthesis of 2,2'-(cyclohexane-1,1-diylbis(4,1-phenylene))bis(4,4,5,5-tetramethyl-1,3,2-dioxaborolane), M3

Compound 2 (1.8 g, 4.6 mmol) was dissolved into 60 mL of 1,4-dioxane in a 250 mL two-neck round bottom flask; potassium acetate (KOAc) (3.16 g, 32.2 mmol), 4,4,4',4',5,5,5',5'-octamethyl-2,2'-bi(1,3,2-dioxaborolane) (4.67 g, 18.4 mmol), and $PdCl_2$(dppf) (0.67 g, 0.92 mmol) were added to the mixture. The reaction solution was protected from light and stirred under a nitrogen atmosphere at 80 °C for 24 h. The resultant was extracted with MC and water. The organic phase was dried with sodium sulfate and then concentrated. The residue was purified by column chromatography (eluent: chloroform) to obtain the final product at a 33 % yield (0.74 g). ^{1}H NMR (400 MHz, $CDCl_3$) δ (ppm) : 7.70 (d, *J* = 7.8 Hz, 4H), 7.28 (d, *J* = 7.8 Hz, 4H), 2.27 (m, 4H), 1.55 (s, 6H), 1.30 (s, 24H). Anal. Calcd. for $C_{30}H_{42}B_2O_4$: C, 73.79; H, 8.67; B, 4.43; O, 13.11. Found: C, 74.22; H, 8.35.

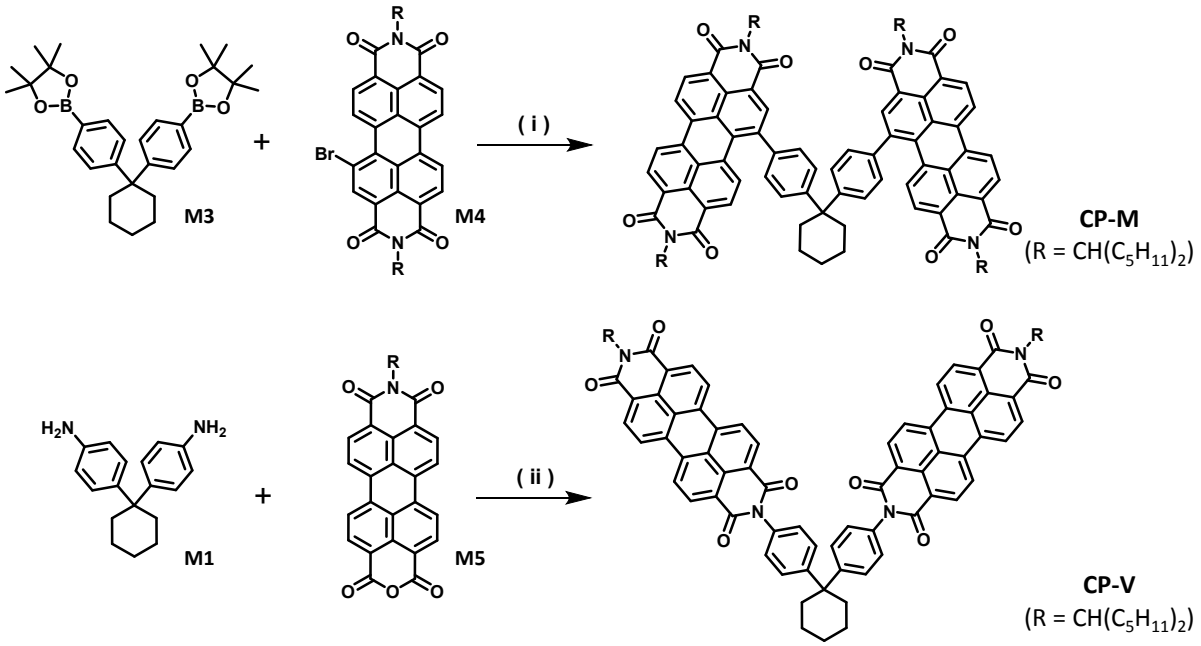

Scheme S2 Synthesis of CP-M and CP-V. (i) $Pd_2(dba)_3$, P(*o*-tolyl)$_3$, K_2CO_3, Aliquat 336 and toluene, 100 °C. (ii) Imidazole, 140 °C.

Synthesis of CP-M

M3 (0.12 g, 0.245 mmol), **M4** (0.43 g, 0.613 mmol), K_2CO_3 (68 mg, 0.49 mmol), $Pd_2(dba)_3$ (11 mg, 9.8 μmol), and a drop of Aliquat 336 were dissolved in 30 mL of degassed toluene in a 100 mL two-neck round bottom flask. The mixture was heated to 90 °C and stirred in a nitrogen atmosphere for 5 h. The resultant was cooled to room temperature and methanol was added. The precipitate were filtered and purified by column chromatography (eluent: MC : hexane = 2:1) to obtain the end product with a 62.7 % yield (0.25 g). ^{1}H NMR (400 MHz, $CDCl_3$) δ (ppm) : 8.70 (m, 10H), 8.15 (m, 2H), 7.95 (m, 2H), 7.50 (m, 8H), 5.20 (m, 4H), 2.45 (m, 4H), 2.05-2.35 (m, 6H), 1.7-1.9 (m, 16H), 1.1-1.4 (m, 48H), 0.7-0.9 (m, 24H). Anal. Calcd for $C_{110}H_{124}N_4O_8$: C, 81.04; H, 7.67; N, 3.44; O, 7.85. Found: C, 80.94; H, 7.54; N, 3.62; O, 7.78. m/z = 1650.4

Synthesis of CP-V

M1 (60 mg, 0.23 mmol), **M5** (0.27 g, 0.05 mmol) and imidazole (5 g) as a solid solvent were added into a Schlenk flask. The mixture was heated to 140 °C in a nitrogen atmosphere for 4

h. The resultant was cooled to room temperature and methanol was poured to quench the reaction. The precipitates from methanol were filtered and purified by column chromatography (eluent: MC : hexane = 1:1) to obtain the end product at a 77.26 % yield (0.23 g). ^{1}H NMR (400 MHz, $CDCl_3$) δ(ppm) : 8.5-8.8 (m, 16H), 7.5 (d, *J*= 8 Hz, 2H), 7.25 (d, *J* = 8 Hz, 2H), 5.20 (m, 2H), 2.40 (m, 3H), 2.25 (m, 4H), 1.85 (m, 3H), 1.55-1.75 (m, 8H), 1.2-1.4 (m, 24H), 0.75-0.85 (m, 12H). Anal. Calcd for $C_{88}H_{80}N_4O_8$: C, 79.97; H, 6.10; N, 4.24; O, 9.68. Found: C, 79.85; H, 6.02; N, 4.18; O, 9.64. m/z = 1343.9

1.2. Measurement

A Thermo Scientific Flash 2000 (Thermo Fisher Scientific) elemental analyzer was used to determine the content of C, H, N, S, and O. The chemical structures of the synthesized compounds were identified by ^{1}H NMR spectroscopy (Varian Mercury 400 MHz spectrometer).

Matrix-assisted laser desorption ionization time of flight (MALDI-TOF) mass spectrometry (LRF20, a Bruker Daltonics) was used to determine the mass of compounds. Samples were prepared by spotting the solution in chloroform with matrix on the target plate.

An HP 8453 photodiode array UV-vis-NIR absorption spectrometer was used to study the UV-vis absorption properties of the solution and film states (λ=190-1100 nm). The film samples were fabricated on washed glass substrates using a 0.7 wt% chloroform solution of small molecules by a spin-coating method.

The electrochemical properties of the synthesized small molecules were examined using cyclic voltammetry (CV, eDAQ EA161). The thin films were fabricated on a Pt wire using a drop-casting method from a chloroform solution. The 0.10 M electrolyte solution was made by dissolving tetrabutylammonium hexafluorophosphate (Bu_4NPF_6) in freshly dried acetonitrile with Pt wire and Ag/AgCl as the counter and reference electrodes, respectively.

Two-dimensional GI-XRD measurements were performed at the 9A (U-SAXS) beamline at the Pohang Accelerator Laboratory (PAL). The energy, pixel size, wavelength, and scanning

interval at the 9A beamline were 11.075 keV, 79.59 μm, 1.11946 Å, and 2θ = 0°–20°, respectively. The scattering vectors, q_{xy} and q_z were parallel and perpendicular to the substrate. The film samples used in the GI-XRD analysis were fabricated by spin coating a small molecule solution and blending the solution with small molecules and PPDT2FBT on a UVO-ozone pretreated wafer.

The surface morphologies of the films were examined by atomic force microscopy (AFM, XE-100 advanced scanning probe microscope, PSIA) with a silicon cantilever. The AFM measurements were performed for the samples fabricated by the same method as for the photovoltaic devices.

Fabrication of Inverted Polymer Solar Cells

Inverted nonfullerene-based polymer solar cells (PSCs) were fabricated with patterned indium-tin-oxide (ITO) glass as an anode. The ITO-coated glass (150 nm-thick, AMG Corp.) with a resistance of 15.0 Ω cm^{-2} was cleaned using acetone, deionized water, and isopropanol (subsequently) for 10 min each by sonication. The ZnO layer (40 nm) was spin-coated on the surface of the washed ITO glass substrates, which were pretreated with UV-ozone for 20 min and then thermally annealed at 200 °C for 1 h. The blending solutions of PPDT2FBT and small molecules (PDI5, CP-M, and CP-V) were spin-coated on top of the previous layer from a chloroform solution with diphenyl ether (DPE) as an additive. Finally, MoO_3 (10 nm) and Ag (100 nm) were deposited onto the photoactive layer through shadow masks using a thermal evaporator to produce a 0.04 cm^2 active area. The current density-voltage (*J*–*V*) characteristics were measured with a Keithley 2400 SourceMeter in the dark and under AM 1.5 G illumination at 100 mW cm^{-2} supplied by a solar simulator (Oriel, 1000 W). An AM 1.5 filter (Oriel) and a neutral density filter were used to reduce the light intensity when necessary to provide a light source that most accurately approximated sunlight. A calibrated broadband optical power meter (Spectra Physics, Model 404) was used to measure the incident light intensity.

Fabrication of hole-only devices (HODs)

The hole-only devices (HODs) were fabricated with a diode structure of glass/ITO/PEDOT:PSS/active layer/Au (PEDOT:PSS = Poly(3,4-ethylenedioxythiophene)-poly(styrenesulfonate)). ITO-coated glass substrates were washed using the same method as for the fabrication of the photovoltaic cells. A PEDOT:PSS thin layer was spin-coated on the surface of the ITO substrates at 4000 rpm for 40 s. The spin-coated substrates were thermally annealed at 150 °C for 15 min. The blending solutions were spin-coated at 2000 rpm for 40 min onto the PEDOT:PSS layer at optimized conditions for photovoltaic cells. Finally, Au (100 nm) was deposited onto the photoactive layer through shadow masks using a thermal evaporator. The devices were tested by a Keithley 2400 source emitter by measuring the current-voltage curve in the range of 0-10 V. The charge carrier mobilities were calculated using the space-charge limited current (SCLC) model.

Fabrication of electron-only devices (EODs)

The electron-only devices (EODs) were fabricated with a diode structure of glass/ITO/ZnO/active layer/LiF/Al. The ITO-coated glass substrates were washed with the same method used for the fabrication of the HODs. A ZnO layer was spin-coated onto the surface of the ITO substrates at 3000 rpm for 40 s. The spin-coated substrates were thermally annealed at 200 °C for 1 h. The blending solutions were spin-coated at 2000 rpm for 40 min onto the ZnO layer at optimized conditions for photovoltaic cells. Finally, LiF (1 nm) and Al (100 nm) were deposited onto the photoactive layer through shadow masks using a thermal evaporator. The devices were tested using the same method as for the HODs.

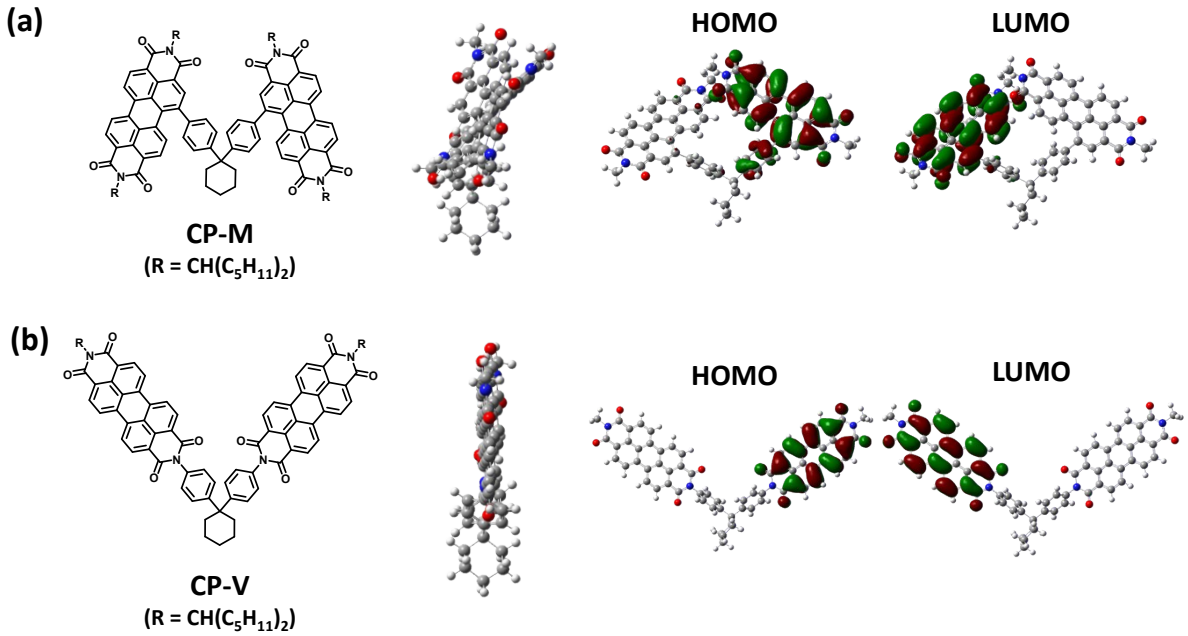

Fig. S1 Molecular structures and DFT calculations of (a) CP-M and (b) CP-V.

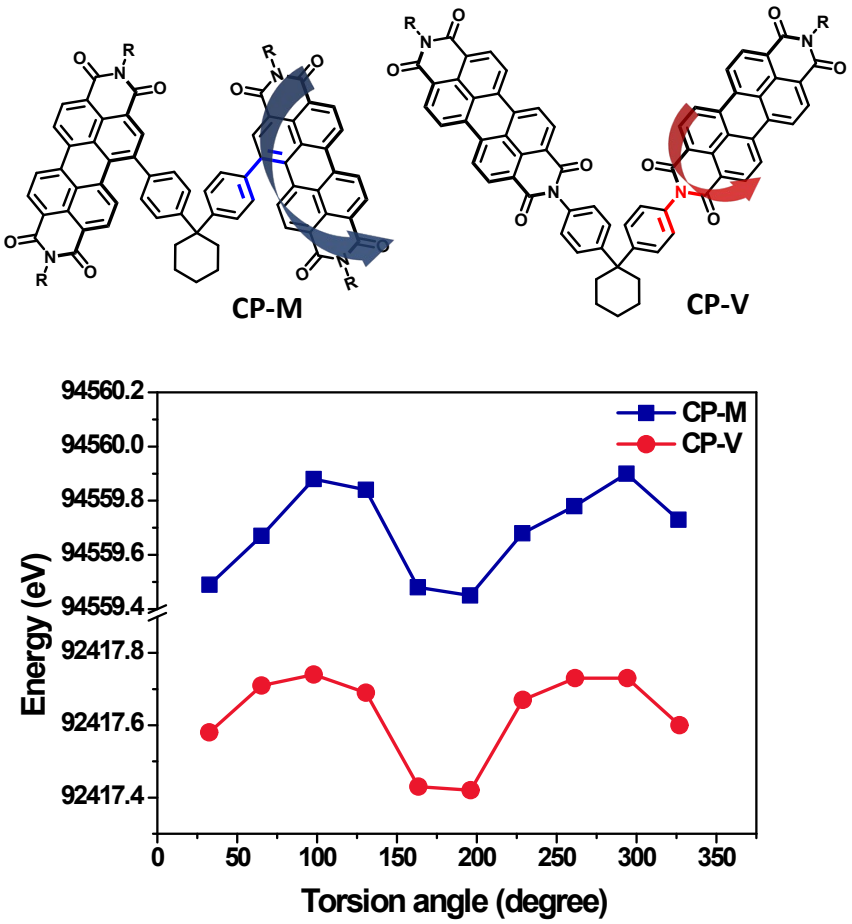

Fig. S2 Torsional energy profiles with respect to the torsional angles between the PDI segments and 1,1-diphenylcyclohexane.

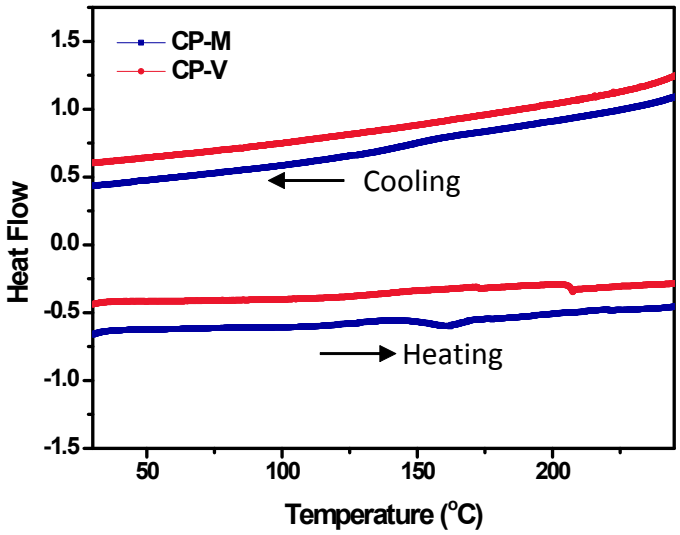

Fig. S3 Differential scanning calorimetry heating and cooling thermograms of CP-M and CP-V.

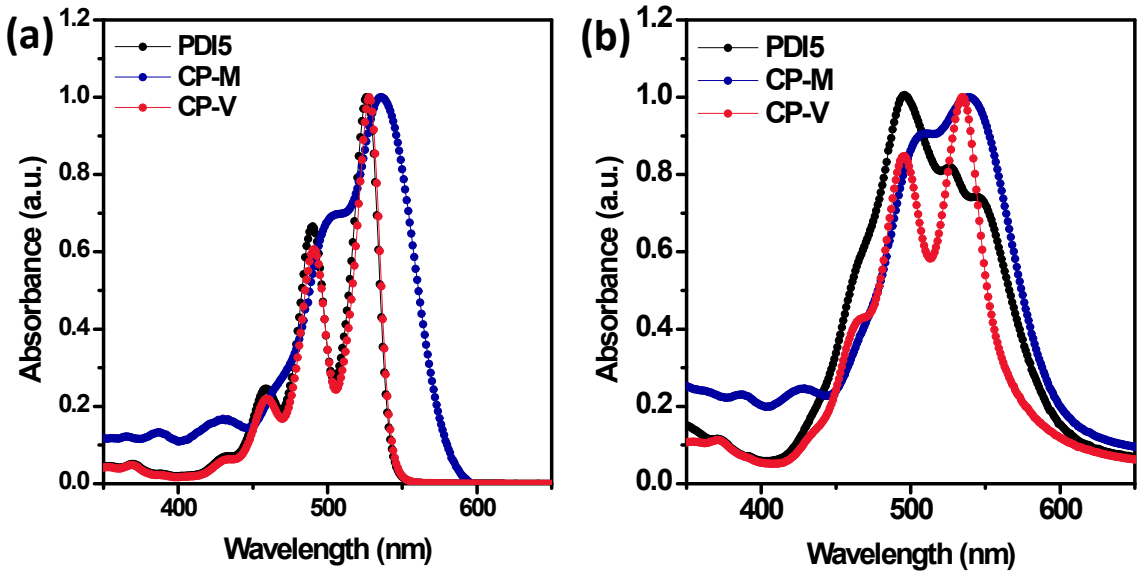

Fig. S4 UV-visible absorption spectra of PDI5, CP-M, and CP-V (a) solutions (in $CHCl_3$) and (b) films.

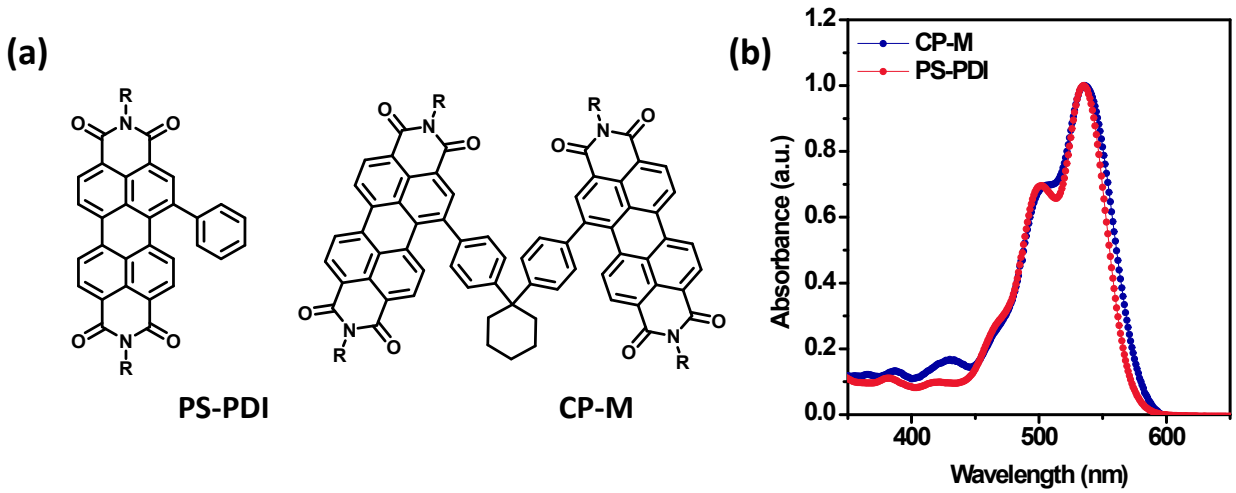

Fig. S5 (a) The structures of PS-PDI and CP-M. (b) UV-Visible absorption spectra of PS-PDI and CP-M solutions in $CHCl_3$.

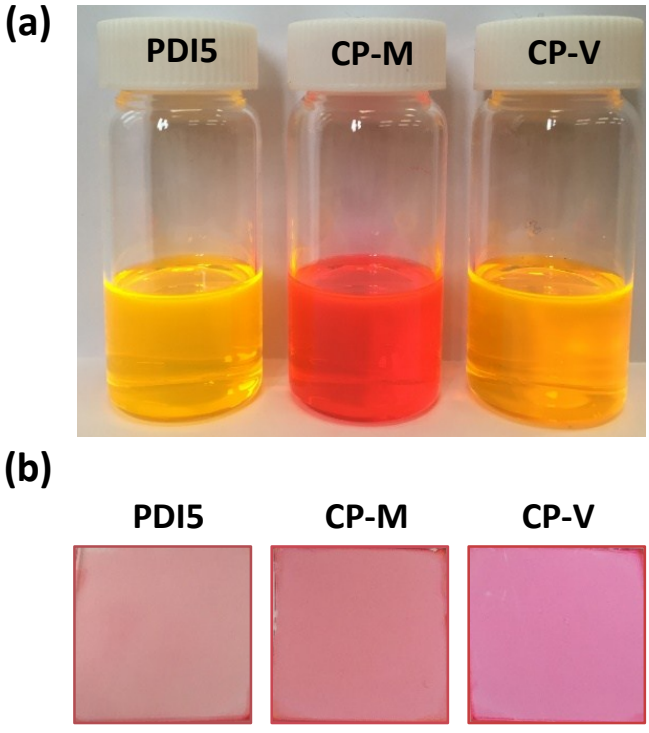

Fig. S6 Photographs of PDI5, CP-M, and CP-V solutions (in $CHCl_3$) and films.

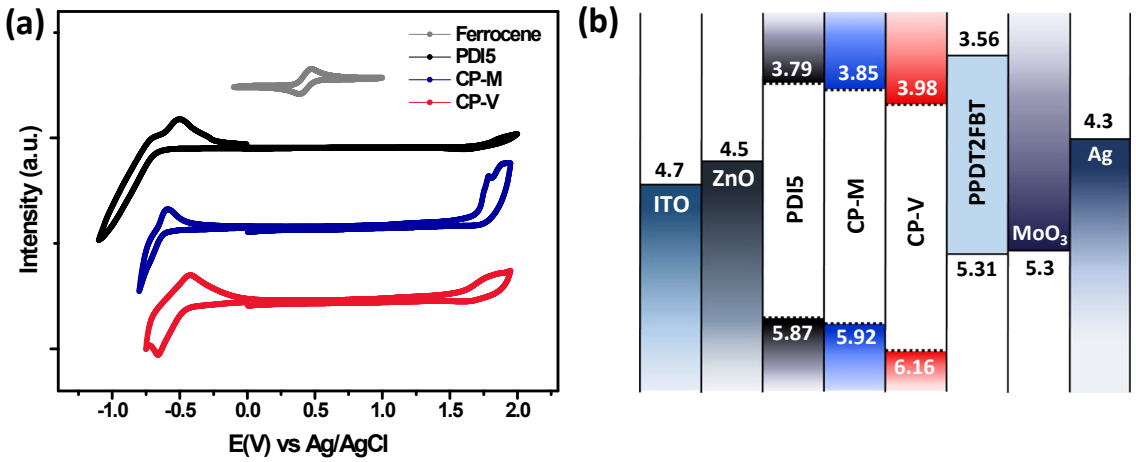

Fig. S7 (a) Cyclic voltammograms of PDI5, CP-M, CP-V, and the ferrocene standard. (b) Configurations of the inverted polymer solar cells with the molecular orbitals of PDI5, CP-M, CP-V, and PPDT2FBT.

Table S1. Physical, optical and electrochemical properties of PPDT2FBT, PDI5, CP-M and CP-V.

	ε (M^{-1} cm^{-1})	λ_{peak}[a] (nm)	λ_{peak}[b] (nm)	$\lambda_{cut\ off}$ (nm)	E_g^{opt} (eV)	E_{ox}^{onset} (V)[b]	E_{red}^{onset} (V)	Energy levels	
								HOMO (eV)	LUMO (eV)
PDI5	9.0×10^4	490, 526	496	543[a], 596[b]	2.28[a], 2.08[b]	1.69	-0.65	-5.87[d]	-3.79[c]
CP-M	14.8×10^4	491, 536	539	583[a], 600[b]	2.13[a], 2.07[b]	1.70	-0.59	-5.92[d]	-3.85[c]
CP-V	23.2×10^4	528	535	543[a], 568[b]	2.28[a], 2.18[b]	1.71	-0.46	-6.16[d]	-3.98[c]

[a] solution [b] film [c] The values were obtained from cyclic voltammograms. *sample: film on Pt electrode.
[d] LUMO(eV) – E_g^{opt}(eV), [e] The optical bandgaps were obtained from absorption spectra of film samples.

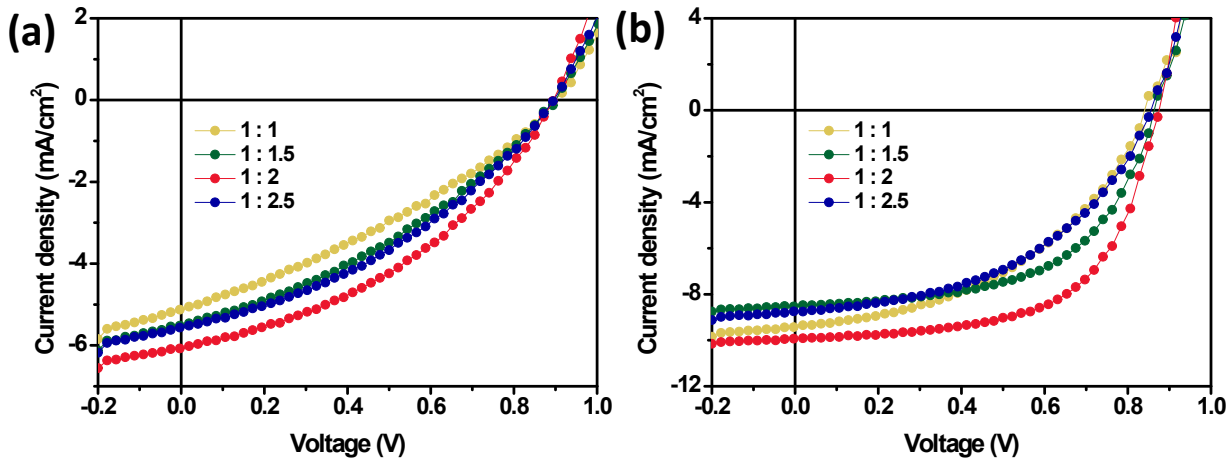

Fig. S8 *J–V* characteristics of the BHJ PSCs with respect to the ratio of p:n. (a) PPDT2FBT:CP-M and PPDT2FBT:CP-V. *Inverted solar cell: ITO/ZnO/Active layer/MoO_3/Ag.

Table S2. Performances of the PSC devices fabricated from CP-M and CP-V with PPDT2FBT.

	p : n	V_{oc} (V)	J_{sc} (mA/cm^2)	FF	PCE (%)
PPDT2FBT : CP-M	1 : 1	0.89	4.66	31.28	1.29
	1 : 1.5	0.89	5.49	35.62	1.74
	1 : 2	0.89	6.04	39.84	2.14
	1 : 2.5	0.89	5.55	37.06	1.84
PPDT2FBT : CP-V	1 : 1	0.84	9.38	45.26	3.58
	1 : 1.5	0.87	8.50	56.16	4.14
	1 : 2	0.87	10.04	60.16	5.28
	1 : 2.5	0.85	8.74	47.62	3.56

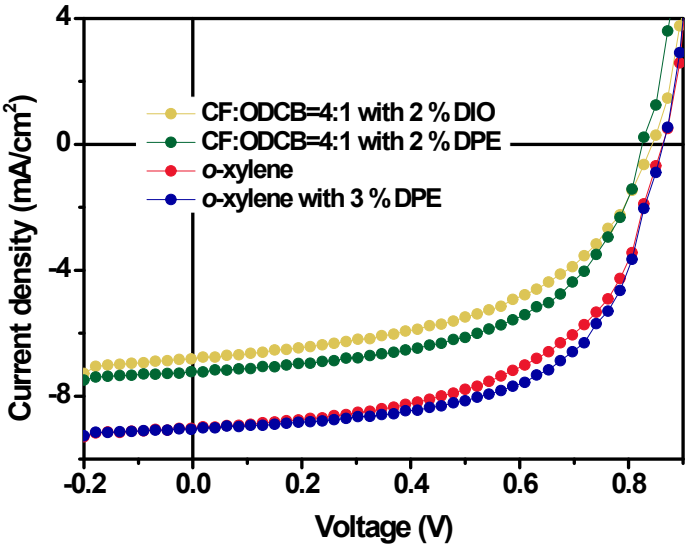

Fig. S9 *J–V* characteristics of the BHJ PSCs with PPDT2FBT:CP-V *Inverted solar cell: ITO/ZnO/Active layer/MoO_3/Ag.

Table S3. Performances of the PSC devices fabricated from CP-V with PPDT2FBT.

		p : n	V_{oc} (V)	J_{sc} (mA/cm²)	FF	PCE (%)
PPDT2FBT : CP-V	CF:ODCB=4:1	DIO 2	0.84	6.80	50.84	2.91
	CF:ODCB=4:1	DPE 2	0.83	7.22	55.15	3.30
	O-xylene	-	0.86	9.00	55.39	4.30
	O-xylene	DPE 3	0.86	9.03	59.97	4.68

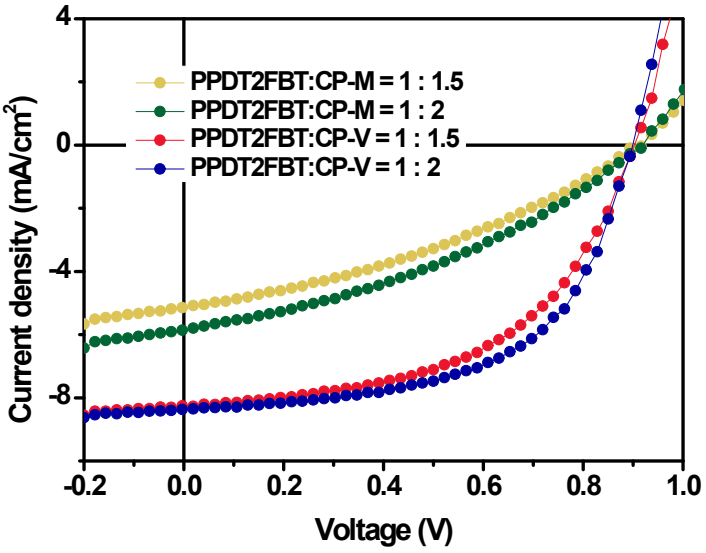

Fig. S10 *J–V* characteristics of BHJ PSCs with PPDT2FBT:CP-M and PPDT2FBT:CP-V. *Conventional solar cell: ITO/PEDOT:PSS(4083)/Active layer/LiF/Al.

Table S4. Performances of the PSC devices fabricated from CP-M and CP-V with PPDT2FBT.

	p : n	V_{oc} (V)	J_{sc} (mA/cm^2)	FF	PCE (%)
PPDT2FBT : CP-M	1:1.5	0.91	5.13	35.42	1.65
	1:2	0.91	5.82	36.35	1.92
PPDT2FBT : CP-V	1:1.5	0.90	8.25	52.31	3.89
	1:2	0.90	8.37	57.04	4.30

*Conventional solar cell: ITO/PEDOT:PSS(4083)/Active layer/LiF/Al.

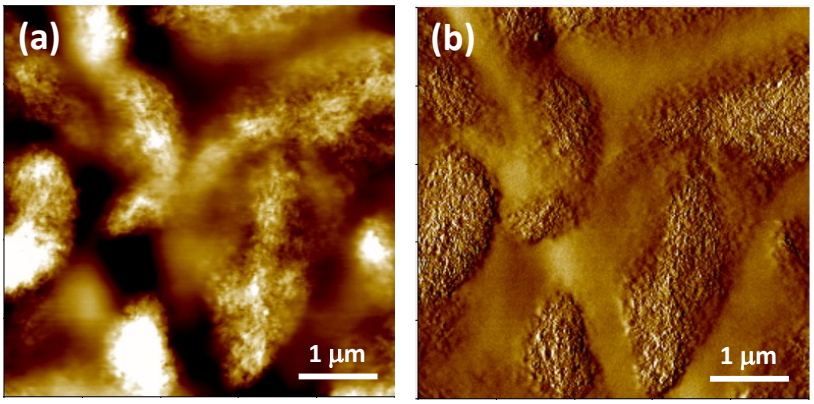

Fig. S11 AFM height images (5 μm × 5 μm) of the blended films: (a) topography image of the PDI5 blending films with PPDT2FBT and (b) phase image of the PDI5 blending films with PPDT2FBT.

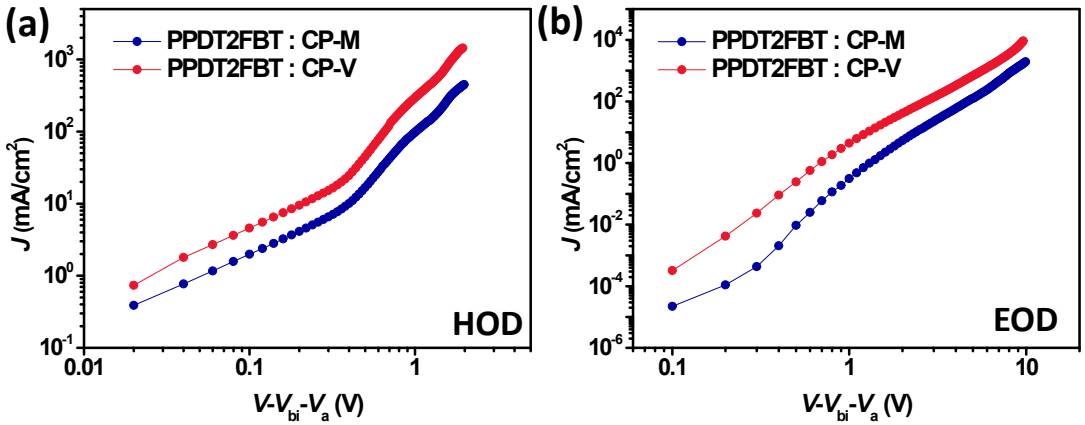

Fig. S12 Current-voltage characteristics of the SCLC devices of PPDT2FBT:CP-M and PPDT2FBT:CP-V blends; (a) hole only devices (HOD) and (b) electron only devices (EOD).

Table S5. Measured electron and hole mobility of the SCLC devices of the PPDT2FBT:CP-M and PPDT2FBT:CP-V blends.

	μ_h (cm²/V s)	μ_e (cm²/V s)	μ_h/μ_e
PPDT2FBT : CP-M	4.26 x 10^{-5}	1.15 x 10^{-6}	37.04
PPDT2FBT : CP-V	1.07 x 10^{-4}	1.39 x 10^{-5}	7.70

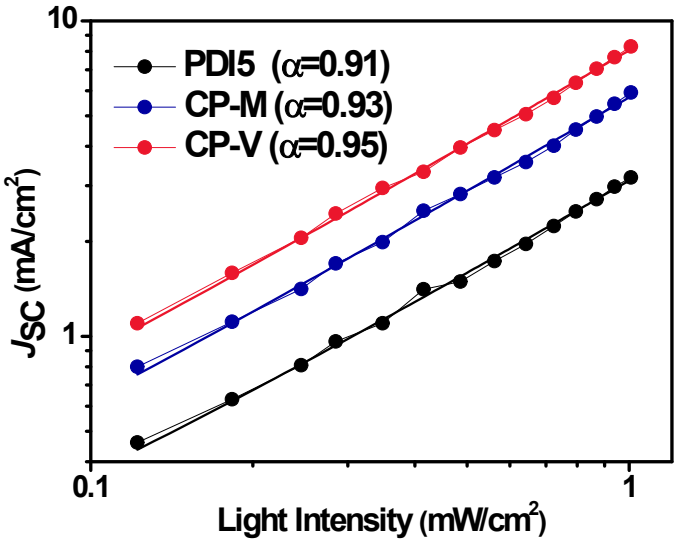

Fig. S13 Photocurrent density versus light intensity for the optimized devices.

The light intensity dependent J_{sc} data are also shown in Fig. S13. From the power law equation of $J_{sc} \propto P^{\alpha}$, α indicates the charge recombination in the PSCs correlating with *FF*. The calculated α values for the PPDT2FBT:CP-M and PPDT2FBT:CP-V devices are 0.93 and 0.95, respectively. The higher α value for the PPDT2FBT:CP-V device indicates a relatively weak bimolecular recombination within the PSCs. Therefore, these results also clearly support smaller non-geminate recombination losses that induce a relatively higher *FF* of CP-V (~ 60 %) than that of CP-M (~ 40 %).

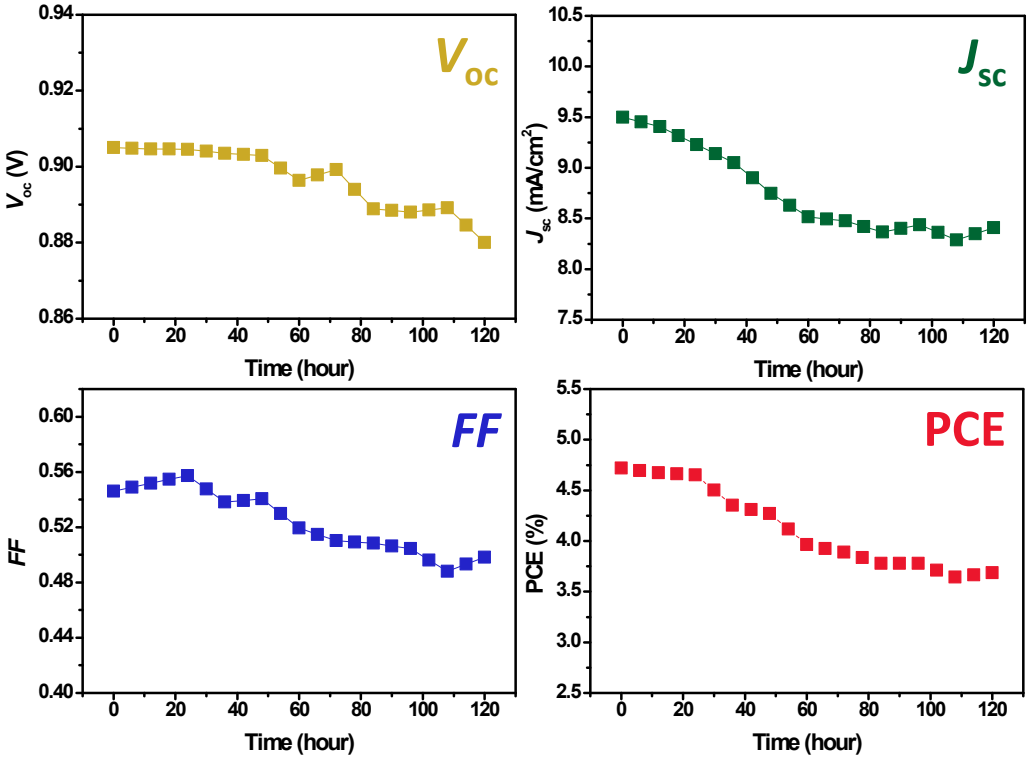

Fig. S13 Photovoltaic parameters (V_{oc}, J_{sc}, *FF* and PCE) versus time of the PPDT2FBT:CP-V solar cell.

We measured the stability of PSC device performance (i.e. stability for 120 hr). The devices made of PPDT2FBT and CP-V were stored at room temperature in air. The device parameters were attained and shown in Fig. S13. In brief, 20% decrease of initial PCE was observed after storing the device at room temperature for 120 hr.

Reference

1. M. H. Yi, W. Huang, M. Y. Jin and K. Y. C, *Macromolecules,* 1997, **30**, 5606.

2. J. Lee , R. Singh , D. H. Sin , H. G. Kim , K. C. Song and K. Cho, *Adv. Mater*. 2016, **28**, 69.

3. S. Rajaram, R. Shivanna, S. K. Kandappa, and K. S. Narayan, *J. Phys. Chem. Lett*. 2012, **3**, 2405.

4. B. V. Veller, D. Robinson and T. M. Swager, *Angew. Chem. Int. Ed*., 2012, **51**, 1182.